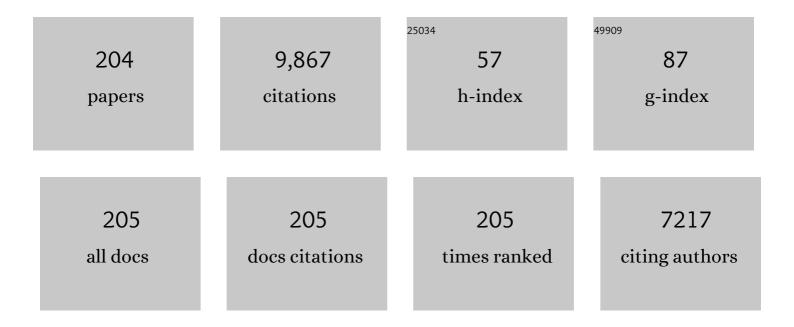
Sang Sub Kim

List of Publications by Year in descending order

Source: https://exaly.com/author-pdf/915219/publications.pdf Version: 2024-02-01



#	Article	IF	CITATIONS
1	Highly conjugated three-dimensional van der Waals heterostructure-based nanocomposite films for ultrahigh-responsive TEA gas sensors at room temperature. Journal of Materials Chemistry A, 2022, 10, 2995-3008.	10.3	20
2	Counter-Intuitive Magneto-Water-Wetting Effect to CO2 Adsorption at Room Temperature Using MgO/Mg(OH)2 Nanocomposites. Materials, 2022, 15, 983.	2.9	2
3	Gate-controlled gas sensor utilizing 1D–2D hybrid nanowires network. IScience, 2022, 25, 103660.	4.1	4
4	Room temperature NO2 sensing performance of a-C-decorated TeO2 nanowires. Sensors and Actuators B: Chemical, 2022, 363, 131853.	7.8	12
5	State-of-the-Art Research on Chemiresistive Gas Sensors in Korea: Emphasis on the Achievements of the Research Labs of Professors Hyoun Woo Kim and Sang Sub Kim. Sensors, 2022, 22, 61.	3.8	5
6	Resistive-Based Gas Sensors Using Quantum Dots: A Review. Sensors, 2022, 22, 4369.	3.8	20
7	Fracture Behavior of Ion-Nitrided AISI 4140 Steel in accordance with Variable Applied Current Density. Advances in Materials Science and Engineering, 2022, 2022, 1-10.	1.8	1
8	Hydrogen sensing characteristics of Pd-decorated ultrathin ZnO nanosheets. Sensors and Actuators B: Chemical, 2021, 329, 129222.	7.8	35
9	SnO2 nanowires decorated by insulating amorphous carbon layers for improved room-temperature NO2 sensing. Sensors and Actuators B: Chemical, 2021, 326, 128801.	7.8	32
10	Functionalization of zirconium-based metal–organic frameworks for gas sensing applications. Journal of Hazardous Materials, 2021, 403, 124104.	12.4	42
11	Recent advances in energy-saving chemiresistive gas sensors: A review. Nano Energy, 2021, 79, 105369.	16.0	282
12	Boosting the sensing properties of resistive-based gas sensors by irradiation techniques: a review. Nanoscale, 2021, 13, 4728-4757.	5.6	33
13	Reduced Graphene Oxide (rGO)-Loaded Metal-Oxide Nanofiber Gas Sensors: An Overview. Sensors, 2021, 21, 1352.	3.8	60
14	CsPbl ₃ <i>NC</i> -Sensitized SnO ₂ /Multiple-Walled Carbon Nanotube Self-Assembled Nanomaterials with Highly Selective and Sensitive NH ₃ Sensing Performance at Room Temperature. ACS Applied Materials & Interfaces, 2021, 13, 14447-14457.	8.0	15
15	Synergistic effects of SnO2 and Au nanoparticles decorated on WS2 nanosheets for flexible, room-temperature CO gas sensing. Sensors and Actuators B: Chemical, 2021, 332, 129493.	7.8	79
16	Selective gas detection and quantification using a resistive sensor based on Pd-decorated soda-lime glass. Sensors and Actuators B: Chemical, 2021, 335, 129714.	7.8	10
17	CuxO Nanostructure-Based Gas Sensors for H2S Detection: An Overview. Chemosensors, 2021, 9, 127.	3.6	23
18	Achievement of self-heated sensing of hazardous gases by WS2 (core)–SnO2 (shell) nanosheets. Journal of Hazardous Materials, 2021, 412, 125196.	12.4	17

#	Article	IF	CITATIONS
19	Gas sensing materials roadmap. Journal of Physics Condensed Matter, 2021, 33, 303001.	1.8	49
20	Proton-beam engineered surface-point defects for highly sensitive and reliable NO2 sensing under humid environments. Journal of Hazardous Materials, 2021, 416, 125841.	12.4	34
21	Effect of Ag Addition on the Gas-Sensing Properties of Nanostructured Resistive-Based Gas Sensors: An Overview. Sensors, 2021, 21, 6454.	3.8	30
22	How femtosecond laser irradiation can affect the gas sensing behavior of SnO2 nanowires toward reducing and oxidizing gases. Sensors and Actuators B: Chemical, 2021, 342, 130036.	7.8	8
23	Humidity-resistant gas sensors based on SnO2 nanowires coated with a porous alumina nanomembrane by molecular layer deposition. Sensors and Actuators B: Chemical, 2021, 344, 130302.	7.8	32
24	Chemical-recognition-driven selectivity of SnO2-nanowire-based gas sensors. Nano Today, 2021, 40, 101265.	11.9	25
25	Decoration of multi-walled carbon nanotubes with CuO/Cu2O nanoparticles for selective sensing of H2S gas. Sensors and Actuators B: Chemical, 2021, 344, 130176.	7.8	41
26	Electrowetting-on-dielectric behavior of micro-nano hierarchical SiO2 layers decorated with noble metals. Ceramics International, 2021, 47, 28312-28320.	4.8	5
27	Facile synthesis of metal-organic framework-derived ZnO/CuO nanocomposites for highly sensitive and selective H2S gas sensing. Sensors and Actuators B: Chemical, 2021, 349, 130741.	7.8	47
28	Preparation of n-ZnO/p-Co3O4 heterojunctions from zeolitic imidazolate frameworks (ZIF-8/ZIF-67) for sensing low ethanol concentrations. Sensors and Actuators B: Chemical, 2021, 348, 130684.	7.8	40
29	Porous Si/SnO2 nanowires heterostructures for H2S gas sensing. Ceramics International, 2020, 46, 604-611.	4.8	61
30	Optimization of the surface coverage of metal nanoparticles on nanowires gas sensors to achieve the optimal sensing performance. Sensors and Actuators B: Chemical, 2020, 302, 127196.	7.8	44
31	Enhancement of gas sensing by implantation of Sb-ions in SnO2 nanowires. Sensors and Actuators B: Chemical, 2020, 304, 127307.	7.8	52
32	Variation of shell thickness in ZnO-SnO2 core-shell nanowires for optimizing sensing behaviors to CO, C6H6, and C7H8 gases. Sensors and Actuators B: Chemical, 2020, 302, 127150.	7.8	56
33	Electrowetting-on-dielectric characteristics of ZnO nanorods. Scientific Reports, 2020, 10, 14194.	3.3	15
34	ZnO Nanosheets Modified with Graphene Quantum Dots and SnO ₂ Quantum Nanoparticles for Room-Temperature H ₂ S Sensing. ACS Applied Nano Materials, 2020, 3, 5220-5230.	5.0	53
35	Changes in characteristics of Pt-functionalized RGO nanocomposites by electron beam irradiation for room temperature NO2 sensing. Ceramics International, 2020, 46, 21638-21646.	4.8	19
36	Hybridization of silicon nanowires with TeO2 branch structures and Pt nanoparticles for highly sensitive and selective toluene sensing. Applied Surface Science, 2020, 525, 146620.	6.1	14

#	Article	IF	CITATIONS
37	Realization of selective CO detection by Ni-incorporated metal-organic frameworks. Sensors and Actuators B: Chemical, 2020, 315, 128110.	7.8	30
38	Indium-implantation-induced enhancement of gas sensing behaviors of SnO2 nanowires by the formation of homo-core–shell structure. Sensors and Actuators B: Chemical, 2020, 321, 128475.	7.8	29
39	Interface treatment using amorphous-carbon and its applications. Scientific Reports, 2020, 10, 4093.	3.3	3
40	Pd-decorated Si nano-horns as sensitive and selective hydrogen gas sensors. Materials Research Bulletin, 2020, 132, 110985.	5.2	14
41	Gas-sensing behaviors of TiO2-layer-modified SnO2 quantum dots in self-heating mode and effects of the TiO2 layer. Sensors and Actuators B: Chemical, 2020, 310, 127870.	7.8	26
42	Synthesis of Au/SnO2 nanostructures allowing process variable control. Scientific Reports, 2020, 10, 346.	3.3	2
43	Flexible and low power CO gas sensor with Au-functionalized 2D WS2 nanoflakes. Sensors and Actuators B: Chemical, 2020, 313, 128040.	7.8	80
44	Pd-functionalized core-shell composite nanowires for self-heating, sensitive, and benzene-selective gas sensors. Sensors and Actuators A: Physical, 2020, 308, 112011.	4.1	15
45	Enhanced humidity sensing properties of Fe-doped CeO2 nanoparticles. Journal of Materials Science: Materials in Electronics, 2020, 31, 8815-8824.	2.2	4
46	Exploration of ZrO2-shelled nanowires for chemiresistive detection of NO2 gas. Sensors and Actuators B: Chemical, 2020, 319, 128309.	7.8	23
47	Effect of Noble Metals on Hydrogen Sensing Properties of Metal Oxide-based Gas Sensors. Journal of Sensor Science and Technology, 2020, 29, 365-368.	0.2	8
48	Atomic‣ayered Tungsten Diselenideâ€Based Porous 3D Architecturing for Highly Sensitive Chemical Sensors. Physica Status Solidi - Rapid Research Letters, 2019, 13, 1900340.	2.4	11
49	Dimethylenebis-(tetra-decyldimethylammonium Bromide)-Driven Metal Nanoparticles: Hg2+ Sensing a Competency. ACS Omega, 2019, 4, 13782-13789.	3.5	2
50	Role of Ruthenium in the Dielectric, Magnetic Properties of Nickel Ferrite (Ru–NiFe ₂ O ₄) Nanoparticles and Their Application in Hydrogen Sensors. ACS Omega, 2019, 4, 12919-12926.	3.5	26
51	Improvement of NO2 Sensing Properties in Pd Functionalized Reduced Graphene Oxides by Electron-Beam Irradiation. Frontiers in Materials, 2019, 6, .	2.4	18
52	Fast Semiconductor–Metal Bidirectional Transition by Flame Chemical Vapor Deposition. ACS Omega, 2019, 4, 11824-11831.	3.5	3
53	Incorporation of metal nanoparticles in soda-lime glass sensors for enhancing selective sensing. Sensors and Actuators B: Chemical, 2019, 296, 126673.	7.8	11
54	Sub-ppm Formaldehyde Detection by n-n TiO2@SnO2 Nanocomposites. Sensors, 2019, 19, 3182.	3.8	32

#	Article	IF	CITATIONS
55	Atomic layer deposition (ALD) on inorganic or polymeric membranes. Journal of Applied Physics, 2019, 126, .	2.5	36
56	Gas Sensing Properties of Mg-Incorporated Metal–Organic Frameworks. Sensors, 2019, 19, 3323.	3.8	20
57	New type of doping effect via metallization of surface reduction in SnO2. Scientific Reports, 2019, 9, 8129.	3.3	3
58	ppb-Level Selective Hydrogen Gas Detection of Pd-Functionalized In2O3-Loaded ZnO Nanofiber Gas Sensors. Sensors, 2019, 19, 4276.	3.8	39
59	Realization of H2S sensing by Pd-functionalized networked CuO nanowires in self-heating mode. Sensors and Actuators B: Chemical, 2019, 299, 126965.	7.8	54
60	Room-temperature NO2 sensor based on electrochemically etched porous silicon. Journal of Alloys and Compounds, 2019, 811, 151975.	5.5	26
61	Co3O4-loaded ZnO nanofibers for excellent hydrogen sensing. International Journal of Hydrogen Energy, 2019, 44, 27499-27510.	7.1	44
62	Selective H2S sensing without external heat by a synergy effect in self-heated CuO-functionalized SnO2-ZnO core-shell nanowires. Sensors and Actuators B: Chemical, 2019, 300, 126981.	7.8	42
63	Promotional effects of ZnO-branching and Au-functionalization on the surface of SnO2 nanowires for NO2 sensing. Journal of Alloys and Compounds, 2019, 786, 27-39.	5.5	56
64	An overview on how Pd on resistive-based nanomaterial gas sensors can enhance response toward hydrogen gas. International Journal of Hydrogen Energy, 2019, 44, 20552-20571.	7.1	91
65	Low-Voltage-Driven Sensors Based on ZnO Nanowires for Room-Temperature Detection of NO ₂ and CO Gases. ACS Applied Materials & Interfaces, 2019, 11, 24172-24183.	8.0	74
66	Realization of Au-decorated WS2 nanosheets as low power-consumption and selective gas sensors. Sensors and Actuators B: Chemical, 2019, 296, 126659.	7.8	81
67	Incorporation of Pt Nanoparticles on the Surface of TeO ₂ -Branched Porous Si Nanowire Structures for Enhanced Room-Temperature Gas Sensing. Journal of Nanoscience and Nanotechnology, 2019, 19, 6647-6655.	0.9	3
68	Pd functionalization on ZnO nanowires for enhanced sensitivity and selectivity to hydrogen gas. Sensors and Actuators B: Chemical, 2019, 297, 126693.	7.8	70
69	Enhancement of CO and NO2 sensing in n-SnO2-p-Cu2O core-shell nanofibers by shell optimization. Journal of Hazardous Materials, 2019, 376, 68-82.	12.4	59
70	Gasochromic WO3 Nanostructures for the Detection of Hydrogen Gas: An Overview. Applied Sciences (Switzerland), 2019, 9, 1775.	2.5	49
71	Toluene- and benzene-selective gas sensors based on Pt- and Pd-functionalized ZnO nanowires in self-heating mode. Sensors and Actuators B: Chemical, 2019, 294, 78-88.	7.8	107
72	Design of supersensitive and selective ZnO-nanofiber-based sensors for H2 gas sensing by electron-beam irradiation. Sensors and Actuators B: Chemical, 2019, 293, 210-223.	7.8	103

#	Article	IF	CITATIONS
73	Selective H2S-sensing performance of Si nanowires through the formation of ZnO shells with Au functionalization. Sensors and Actuators B: Chemical, 2019, 289, 1-14.	7.8	35
74	Highly efficient hydrogen sensors based on Pd nanoparticles supported on boron nitride coated ZnO nanowires. Journal of Materials Chemistry A, 2019, 7, 8107-8116.	10.3	114
75	Enhanced Hydrogen Detection in ppb-Level by Electrospun SnO2-Loaded ZnO Nanofibers. Sensors, 2019, 19, 726.	3.8	27
76	Nanostructured Semiconducting Metal Oxide Gas Sensors for Acetaldehyde Detection. Chemosensors, 2019, 7, 56.	3.6	26
77	Resistive gas sensors based on metal-oxide nanowires. Journal of Applied Physics, 2019, 126, .	2.5	148
78	A Novel X-Ray Radiation Sensor Based on Networked SnO2 Nanowires. Applied Sciences (Switzerland), 2019, 9, 4878.	2.5	10
79	Improving the hydrogen sensing properties of SnO2 nanowire-based conductometric sensors by Pd-decoration. Sensors and Actuators B: Chemical, 2019, 285, 358-367.	7.8	93
80	Combination of Pd loading and electron beam irradiation for superior hydrogen sensing of electrospun ZnO nanofibers. Sensors and Actuators B: Chemical, 2019, 284, 628-637.	7.8	56
81	Predictive gas sensor based on thermal fingerprints from Pt-SnO2 nanowires. Sensors and Actuators B: Chemical, 2019, 281, 670-678.	7.8	63
82	Enhancement of H2S sensing performance of p-CuO nanofibers by loading p-reduced graphene oxide nanosheets. Sensors and Actuators B: Chemical, 2019, 281, 453-461.	7.8	71
83	Synthesis, Characterization and Gas-Sensing Properties of Pristine and SnS2 Functionalized TeO2 Nanowires. Metals and Materials International, 2019, 25, 805-813.	3.4	15
84	Design and fabrication of highly selective H2 sensors based on SIM-1 nanomembrane-coated ZnO nanowires. Sensors and Actuators B: Chemical, 2018, 264, 410-418.	7.8	37
85	Super anticorrosion of aluminized steel by a controlled Mg supply. Scientific Reports, 2018, 8, 3760.	3.3	3
86	Dual sensitization of MWCNTs by co-decoration with p- and n-type metal oxide nanoparticles. Sensors and Actuators B: Chemical, 2018, 264, 150-163.	7.8	23
87	CuO–TiO2 p–n core–shell nanowires: Sensing mechanism and p/n sensing-type transition. Applied Surface Science, 2018, 448, 489-497.	6.1	44
88	Low power-consumption CO gas sensors based on Au-functionalized SnO2-ZnO core-shell nanowires. Sensors and Actuators B: Chemical, 2018, 267, 597-607.	7.8	118
89	Superhydrophobic and oleophilic microâ€nano hierarchical Pdâ€decorated SiO 2 layers. Journal of the American Ceramic Society, 2018, 101, 3817-3829.	3.8	5
90	Converting the Conducting Behavior of Graphene Oxides from n-Type to p-Type via Electron-Beam Irradiation. ACS Applied Materials & Interfaces, 2018, 10, 7324-7333.	8.0	18

#	Article	IF	CITATIONS
91	Porous Si nanowires for highly selective room-temperature NO ₂ gas sensing. Nanotechnology, 2018, 29, 294001.	2.6	23
92	Gas sensing properties of standard soda-lime glass. Sensors and Actuators B: Chemical, 2018, 266, 344-353.	7.8	12
93	Resistive-based gas sensors for detection of benzene, toluene and xylene (BTX) gases: a review. Journal of Materials Chemistry C, 2018, 6, 4342-4370.	5.5	255
94	Room Temperature Hard Radiation Detectors Based on Solid State Compound Semiconductors: An Overview. Electronic Materials Letters, 2018, 14, 261-287.	2.2	44
95	Sensing behavior to ppm-level gases and synergistic sensing mechanism in metal-functionalized rGO-loaded ZnO nanofibers. Sensors and Actuators B: Chemical, 2018, 255, 1884-1896.	7.8	100
96	Fabrication and gas sensing properties of vertically aligned Si nanowires. Applied Surface Science, 2018, 427, 215-226.	6.1	41
97	SnO2 (n)-NiO (p) composite nanowebs: Gas sensing properties and sensing mechanisms. Sensors and Actuators B: Chemical, 2018, 258, 204-214.	7.8	115
98	How shell thickness can affect the gas sensing properties of nanostructured materials: Survey of literature. Sensors and Actuators B: Chemical, 2018, 258, 270-294.	7.8	117
99	Significant Enhancement of Hydrogen-Sensing Properties of ZnO Nanofibers through NiO Loading. Nanomaterials, 2018, 8, 902.	4.1	41
100	High-Performance Nanowire Hydrogen Sensors by Exploiting the Synergistic Effect of Pd Nanoparticles and Metal–Organic Framework Membranes. ACS Applied Materials & Interfaces, 2018, 10, 34765-34773.	8.0	135
101	Selective NO2 sensor based on Bi2O3 branched SnO2 nanowires. Sensors and Actuators B: Chemical, 2018, 274, 356-369.	7.8	75
102	Resistance-based H2S gas sensors using metal oxide nanostructures: A review of recent advances. Journal of Hazardous Materials, 2018, 357, 314-331.	12.4	298
103	Electrowetting on dielectric (EWOD) properties of Teflon-coated electrosprayed silica layers in air and oil media and the influence of electric leakage. Journal of Materials Chemistry C, 2018, 6, 6808-6815.	5.5	19
104	Enhancement of the benzene-sensing performance of Si nanowires through the incorporation of TeO2 heterointerfaces and Pd-sensitization. Sensors and Actuators B: Chemical, 2017, 244, 1085-1097.	7.8	35
105	Synthesis and Selective Sensing Properties of rGO/Metal-Coloaded SnO2 Nanofibers. Journal of Electronic Materials, 2017, 46, 3531-3541.	2.2	30
106	Enhancement of gas sensing properties by the functionalization of ZnO-branched SnO2 nanowires with Cr2O3 nanoparticles. Sensors and Actuators B: Chemical, 2017, 249, 656-666.	7.8	56
107	Extremely sensitive and selective sub-ppm CO detection by the synergistic effect of Au nanoparticles and core–shell nanowires. Sensors and Actuators B: Chemical, 2017, 249, 177-188.	7.8	63
108	Self-heating effects on the toluene sensing of Pt-functionalized SnO2–ZnO core–shell nanowires. Sensors and Actuators B: Chemical, 2017, 251, 781-794.	7.8	41

#	Article	IF	CITATIONS
109	Synthesis, characterization and gas sensing properties of ZnO-decorated MWCNTs. Applied Surface Science, 2017, 413, 242-252.	6.1	86
110	Optimization and gas sensing mechanism of n-SnO2-p-Co3O4 composite nanofibers. Sensors and Actuators B: Chemical, 2017, 248, 500-511.	7.8	116
111	Synthesis of zinc oxide semiconductors-graphene nanocomposites by microwave irradiation for application to gas sensors. Sensors and Actuators B: Chemical, 2017, 249, 590-601.	7.8	142
112	Microwave-Assisted Synthesis of Graphene–SnO ₂ Nanocomposites and Their Applications in Gas Sensors. ACS Applied Materials & Interfaces, 2017, 9, 31667-31682.	8.0	149
113	Ultra-sensitive benzene detection by a novel approach: Core-shell nanowires combined with the Pd-functionalization. Sensors and Actuators B: Chemical, 2017, 239, 578-585.	7.8	43
114	Optimization of metal nanoparticle amount on SnO2 nanowires to achieve superior gas sensing properties. Sensors and Actuators B: Chemical, 2017, 238, 374-380.	7.8	30
115	Modification of SnO2 Nanowires with TeO2 Branches and Their Enhanced Gas Sensing. Proceedings (mdpi), 2017, 1, 404.	0.2	3
116	Synthesis and gas sensing properties of membrane template-grown hollow ZnO nanowires. Nano Convergence, 2017, 4, 27.	12.1	17
117	Electrospun Metal Oxide Composite Nanofibers Gas Sensors: A Review. Journal of the Korean Ceramic Society, 2017, 54, 366-379.	2.3	90
118	Growth of Networked TiO2 Nanowires for Gas-Sensing Applications. Journal of Nanoscience and Nanotechnology, 2016, 16, 11580-11585.	0.9	10
119	Improvement of Toluene-Sensing Performance of SnO2 Nanofibers by Pt Functionalization. Sensors, 2016, 16, 1857.	3.8	21
120	Selective Improvement of NO ₂ Gas Sensing Behavior in SnO ₂ Nanowires by Ion-Beam Irradiation. ACS Applied Materials & Interfaces, 2016, 8, 13646-13658.	8.0	110
121	Crystallinity dependent gas-sensing abilities of ZnO hollow fibers. Metals and Materials International, 2016, 22, 942-946.	3.4	11
122	Grain-Size-Tuned Highly H ₂ -Selective Chemiresistive Sensors Based on ZnO–SnO ₂ Composite Nanofibers. ACS Applied Materials & Interfaces, 2016, 8, 2486-2494.	8.0	83
123	Highly Selective Sensing of CO, C ₆ H ₆ , and C ₇ H ₈ Gases by Catalytic Functionalization with Metal Nanoparticles. ACS Applied Materials & Interfaces, 2016, 8, 7173-7183.	8.0	75
124	MOF-Based Membrane Encapsulated ZnO Nanowires for Enhanced Gas Sensor Selectivity. ACS Applied Materials & Interfaces, 2016, 8, 8323-8328.	8.0	346
125	Realization of ppm-level CO detection with exceptionally high sensitivity using reduced graphene oxide-loaded SnO ₂ nanofibers with simultaneous Au functionalization. Chemical Communications, 2016, 52, 3832-3835.	4.1	40
126	Selective detection of low concentration toluene gas using Pt-decorated carbon nanotubes sensors. Sensors and Actuators B: Chemical, 2016, 227, 157-168.	7.8	82

#	Article	IF	CITATIONS
127	Optimum shell thickness and underlying sensing mechanism in p–n CuO–ZnO core–shell nanowires. Sensors and Actuators B: Chemical, 2016, 222, 249-256.	7.8	64
128	Excellent Carbon Monoxide Sensing Performance of Au-Decorated SnO2 Nanofibers. Korean Journal of Materials Research, 2016, 26, 741-750.	0.2	19
129	Low Temperature Sensing Properties of Pt Nanoparticle-Functionalized Networked ZnO Nanowires. Journal of Nanoscience and Nanotechnology, 2015, 15, 330-333.	0.9	14
130	Growth and sensing properties of networked p-CuO nanowires. Sensors and Actuators B: Chemical, 2015, 212, 190-195.	7.8	76
131	Highly sensitive and selective H2 sensing by ZnO nanofibers and the underlying sensing mechanism. Journal of Hazardous Materials, 2015, 286, 229-235.	12.4	104
132	Extraordinary Improvement of Gas-Sensing Performances in SnO ₂ Nanofibers Due to Creation of Local <i>p</i> – <i>n</i> Heterojunctions by Loading Reduced Graphene Oxide Nanosheets. ACS Applied Materials & Interfaces, 2015, 7, 3101-3109.	8.0	143
133	Striking sensing improvement of n-type oxide nanowires by electronic sensitization based on work function difference. Journal of Materials Chemistry C, 2015, 3, 1521-1527.	5.5	57
134	Realization of ppb-Scale Toluene-Sensing Abilities with Pt-Functionalized SnO ₂ –ZnO Core–Shell Nanowires. ACS Applied Materials & Interfaces, 2015, 7, 17199-17208.	8.0	87
135	Excellent gas detection of ZnO nanofibers by loading with reduced graphene oxide nanosheets. Sensors and Actuators B: Chemical, 2015, 221, 1499-1507.	7.8	112
136	Chemiresistive Sensing Behavior of SnO ₂ (<i>n</i>)–Cu ₂ O (<i>p</i>) Core–Shell Nanowires. ACS Applied Materials & Interfaces, 2015, 7, 15351-15358.	8.0	74
137	Promotion of acceptor formation in SnO2 nanowires by e-beam bombardment and impacts to sensor application. Scientific Reports, 2015, 5, 10723.	3.3	33
138	Nanograins in electrospun oxide nanofibers. Metals and Materials International, 2015, 21, 213-221.	3.4	15
139	Bifunctional Sensing Mechanism of SnO ₂ –ZnO Composite Nanofibers for Drastically Enhancing the Sensing Behavior in H ₂ Gas. ACS Applied Materials & Interfaces, 2015, 7, 11351-11358.	8.0	143
140	Synthesis and room-temperature NO2 sensing properties of Sb2O5 nanowires. Metals and Materials International, 2015, 21, 415-421.	3.4	13
141	An ultra-sensitive hydrogen gas sensor using reduced graphene oxide-loaded ZnO nanofibers. Chemical Communications, 2015, 51, 15418-15421.	4.1	81
142	Growth and structure of Mg-Al spinel nanodonut-decorated MgO nanowires. Metals and Materials International, 2015, 21, 956-961.	3.4	2
143	One-pot synthesis of h-BN fullerenes usinsg a graphene oxide template. Metals and Materials International, 2015, 21, 950-955.	3.4	5
144	Dual Functional Sensing Mechanism in SnO ₂ –ZnO Core–Shell Nanowires. ACS Applied Materials & Interfaces, 2014, 6, 8281-8287.	8.0	125

#	Article	IF	CITATIONS
145	Thermochemical analysis on the growth of NiAl2O4rods. RSC Advances, 2014, 4, 1159-1162.	3.6	1
146	Prominent Reducing Gas-Sensing Performances of <i>n</i> -SnO ₂ Nanowires by Local Creation of <i>p</i> – <i>n</i> Heterojunctions by Functionalization with <i>p</i> -Cr ₂ O ₃ Nanoparticles. ACS Applied Materials & Interfaces, 2014, 6, 17723-17729.	8.0	101
147	A novel approach to improving oxidizing-gas sensing ability of p-CuO nanowires using biased radial modulation of a hole-accumulation layer. Journal of Materials Chemistry C, 2014, 2, 8911-8917.	5.5	35
148	Improvement of gas sensing behavior in reduced graphene oxides by electron-beam irradiation. Sensors and Actuators B: Chemical, 2014, 203, 143-149.	7.8	35
149	Different Directions of Switching of Chromium Oxide Thin Films. Journal of Electronic Materials, 2014, 43, 2747-2753.	2.2	6
150	Grain size dependent bandgap shift of SnO2 nanofibers. Metals and Materials International, 2014, 20, 163-167.	3.4	29
151	Control of morphology and orientation of electrochemically grown ZnO nanorods. Metals and Materials International, 2014, 20, 337-342.	3.4	4
152	Mechanism and prominent enhancement of sensing ability to reducing gases in p/n core–shell nanofiber. Nanotechnology, 2014, 25, 175501.	2.6	50
153	Evidence of Ostwald ripening during evolution of micro-scale solid carbon spheres. Scientific Reports, 2014, 4, 3579.	3.3	29
154	Acceptor-Compensated Charge Transport and Surface Chemical Reactions in Au-Implanted SnO2 Nanowires. Scientific Reports, 2014, 4, 4622.	3.3	29
155	Significant change in water contact angle of electrosprayâ€synthesized SiO ₂ films depending on their surface morphology. Surface and Interface Analysis, 2013, 45, 656-660.	1.8	14
156	Microstructure evolution of sputter-deposited Al0.75Mg0.25 alloy films. Metals and Materials International, 2013, 19, 211-215.	3.4	1
157	Micro-nano hierarchical superhydrophobic electrospray-synthesized silica layers. Journal of Colloid and Interface Science, 2013, 392, 376-381.	9.4	33
158	Bi-functional mechanism of H2S detection using CuO–SnO2 nanowires. Journal of Materials Chemistry C, 2013, 1, 5454.	5.5	65
159	NO2-sensing performance of SnO2 microrods by functionalization of Ag nanoparticles. Journal of Materials Chemistry C, 2013, 1, 2834.	5.5	73
160	An approach to detecting a reducing gas by radial modulation of electron-depleted shells in core–shell nanofibers. Journal of Materials Chemistry A, 2013, 1, 13588.	10.3	87
161	Platinum nanoparticle-functionalized tin dioxide nanowires via radiolysis and their sensing capability. Journal of Materials Research, 2012, 27, 1688-1694.	2.6	7
162	Novel growth of CuO-functionalized, branched SnO ₂ nanowires and their application to H ₂ S sensors. Journal Physics D: Applied Physics, 2012, 45, 205301.	2.8	36

#	Article	IF	CITATIONS
163	Surface properties of sol-gel processed TiO2-SiO2 amorphous composite films. Metals and Materials International, 2012, 18, 869-873.	3.4	4
164	NO ₂ gas sensing properties of ZnO sheathed CuO nanorods. Surface and Interface Analysis, 2012, 44, 1534-1537.	1.8	11
165	Synthesis of ferromagnetic nickel ferrite nanofibers via electrospinning with iron acetate as an iron precursor. Metals and Materials International, 2012, 18, 505-508.	3.4	4
166	Synthesis of Hollow Silica Fibers with Porous Walls by Coaxial Electrospinning Method. Journal of the American Ceramic Society, 2012, 95, 553-556.	3.8	23
167	Superhydrophobicity of electrospray-synthesized fluorinated silica layers. Journal of Colloid and Interface Science, 2012, 368, 599-602.	9.4	25
168	Unipolar resistance switching characteristics in a thick ZnO/Cu/ZnO multilayer structure. Journal of the Korean Physical Society, 2012, 60, 1087-1091.	0.7	6
169	Preparation of highly stable TiO2 sols and nanocrystalline TiO2 films via a low temperature sol–gel route. Journal of Sol-Gel Science and Technology, 2012, 61, 77-82.	2.4	31
170	Dependence of gas sensing properties in ZnO nanofibers on size and crystallinity of nanograins. Journal of Materials Research, 2011, 26, 1662-1665.	2.6	28
171	Junction-Tuned SnO ₂ Nanowires and Their Sensing Properties. Journal of Physical Chemistry C, 2011, 115, 12774-12781.	3.1	72
172	Epitaxial Growth of ZnO Films on ZnO-Buffered Al2O3 (0001) in Water at 95°C. Journal of the American Ceramic Society, 2011, 94, 978-981.	3.8	8
173	Tailoring the Number of Junctions per Electrode Pair in Networked <scp>ZnO</scp> Nanowire Sensors. Journal of the American Ceramic Society, 2011, 94, 3922-3926.	3.8	13
174	Synthesis of Highly Crystalline Hollow <scp>TiO</scp> ₂ Fibers Using Atomic Layer Deposition on Polymer Templates. Journal of the American Ceramic Society, 2011, 94, 1974-1977.	3.8	26
175	Significant enhancement of the NO2 sensing capability in networked SnO2 nanowires by Au nanoparticles synthesized via γ-ray radiolysis. Journal of Hazardous Materials, 2011, 193, 243-248.	12.4	62
176	Growth behavior of nanograins in NiO fibers. Materials Chemistry and Physics, 2011, 127, 16-20.	4.0	22
177	Growth kinetics of nanograins in SnO2 fibers and size dependent sensing properties. Sensors and Actuators B: Chemical, 2011, 152, 254-260.	7.8	114
178	A model for the enhancement of gas sensing properties in SnO ₂ –ZnO core–shell nanofibres. Journal Physics D: Applied Physics, 2011, 44, 205403.	2.8	47
179	Stabilization of the anatase phase of Ti1â^'xSnxO2 (x < 0.5) nanofibers. Nano Research, 2010, 3, 256-263.	10.4	15
180	Controlling the size of nanograins in TiO2 nanofibers. Metals and Materials International, 2010, 16, 785-788.	3.4	9

#	ARTICLE	IF	CITATIONS
181	Growth of ZnO Nanobrushes Using a Twoâ€&tep Aqueous Solution Method. Journal of the American Ceramic Society, 2010, 93, 3190-3194.	3.8	8
182	Significant enhancement of the sensing characteristics of In ₂ O ₃ nanowires by functionalization with Pt nanoparticles. Nanotechnology, 2010, 21, 415502.	2.6	69
183	Effects of processing parameters on the synthesis of TiO2 nanofibers by electrospinning. Metals and Materials International, 2009, 15, 95-99.	3.4	26
184	Local electronic structure of phosphorus-doped ZnO films investigated by X-ray absorption near-edge spectroscopy. Applied Physics A: Materials Science and Processing, 2009, 94, 995-998.	2.3	17
185	Growth of Nanograins in Electrospun ZnO Nanofibers. Journal of the American Ceramic Society, 2009, 92, 1691-1694.	3.8	85
186	Synthesis and Gas Sensing Properties of TiO ₂ –ZnO Core‣hell Nanofibers. Journal of the American Ceramic Society, 2009, 92, 2551-2554.	3.8	177
187	The Effects of Growth Temperature on the Fieldâ€Emission Properties of ZnO Nanoneedle Arrays. Journal of the American Ceramic Society, 2009, 92, 2982-2986.	3.8	6
188	Synthesis of SnO ₂ –ZnO core–shell nanofibers via a novel two-step process and their gas sensing properties. Nanotechnology, 2009, 20, 465603.	2.6	241
189	Bi2Sn2O7 nanoparticles attached to SnO2 nanowires and used as catalysts. Chemical Physics Letters, 2008, 456, 193-197.	2.6	48
190	Relative Photoluminescence of ZnO Nanorods Size-Controlled by Changing the Precursor Ratio in Metal Organic Chemical Vapor Deposition. Metals and Materials International, 2008, 14, 357-360.	3.4	9
191	Electrical Properties of Sputtered ZnO Films with Nitrogen and Phosphorous Co-doping. Metals and Materials International, 2008, 14, 471-475.	3.4	3
192	Comment on "Characterization of As-doped, p-type ZnO by x-ray absorption near-edge structure spectroscopy: Theory―[Appl. Phys. Lett. 89, 222113 (2006)]. Applied Physics Letters, 2008, 92, 236101.	3.3	7
193	Investigations of the characteristics of strain-free oxidation on InAlAs epilayer lattice matched to indium phosphide. Applied Physics Letters, 2006, 88, 201914.	3.3	2
194	Electrical transport properties of size-tuned ZnO nanorods. Journal of Materials Research, 2006, 21, 132-136.	2.6	14
195	Piezoelectric effect in epitaxial PbZr1â^'xTixO3 thin films near morphotropic phase boundary region. Journal of Materials Research, 2005, 20, 787-790.	2.6	10
196	Thickness effect of ferroelectric domain switching in epitaxial PbTiO3 thin films on Pt(001)/MgO(001). Applied Physics Letters, 2004, 84, 5085-5087.	3.3	37
197	Heteroepitaxial growth behavior of Mn-doped ZnO thin films on Al2O3 (0001) by pulsed laser deposition. Journal of Applied Physics, 2004, 95, 454-459.	2.5	94
198	Thickness dependence of leakage current behavior in epitaxial (Ba,Sr)TiO3 film capacitors. Journal of Applied Physics, 2003, 93, 1725-1730.	2.5	29

#	Article	IF	CITATIONS
199	Heteroepitaxial growth behavior of SrRuO3/SrTiO3(001) by pulsed laser deposition. Journal of Applied Physics, 2002, 92, 4820-4824.	2.5	6
200	Significant suppression of leakage current in (Ba,Sr)TiO3 thin films by Ni or Mn doping. Journal of Applied Physics, 2002, 92, 2651-2654.	2.5	71
201	Change of growth orientation in Pt films epitaxially grown on MgO(001) substrates by sputtering. Journal of Materials Research, 2002, 17, 2334-2338.	2.6	42
202	Change of conduction mechanism by microstructural variation in Pt/(Ba,Sr)TiO3/Pt film capacitors. Journal of Applied Physics, 2002, 92, 421-425.	2.5	38
203	Structural evolution of epitaxial SrRuO3 thin films grown on SrTiO3(001). Journal of Applied Physics, 2001, 90, 4407-4410.	2.5	20
204	Graphitization of ultrathin amorphous carbon films on Si(001) by Ar+ ion irradiation at ambient temperature. Journal of Applied Physics, 2000, 88, 55-58.	2.5	13